Effects of carbon dioxide on peak mode isotachophoresis: Simultaneous preconcentration and separation†

Tarun K. Khurana and Juan G. Santiago*

Received 4th September 2008, Accepted 10th February 2009
First published as an Advance Article on the web 12th March 2009
DOI: 10.1039/b815460k

We present a method that achieves simultaneous preconcentration and separation of analytes using peak-mode isotachophoresis with a single step injection in simple, off-the-shelf microchannels or capillaries. We leverage ions resulting from dissolved atmospheric carbon dioxid
e to weakly disrupt isotachophoretic preconcentration and induce separation of analyte species. We experimentally study the region between the leading and trailing electrolytes, and individually identify the carbonate and carbamate zones that result from the hydration and carbamation reaction of dissolved atmospheric carbon dioxide, respectively. The width of these zones and the gradient regions between them grow with time and create an electric field gradient that causes analytes to separate. Using this assay, we achieve focusing and separation of a 25 bp DNA ladder in a straight, 34 μm wide microchannel in a single loading step. As a demonstration of the fractionation capabilities of the assay, we show simultaneous preconcentration and separation of a DNA ladder from two proteins, GFP and allophycocyanin.

Introduction

Capillary electrophoresis (CE) is a popular chemical and biological analysis technique widely used on both microchip and capillary format devices.[1,2] CE devices use narrow bore capillaries or shallow microfabricated channels to achieve fast, high efficiency separations; often at the expense of lower detection sensitivity due to shorter optical path lengths. Therefore, preconcentration techniques such as field amplified sample stacking (FASS),[3,4] field amplified sample injection (FASI)[5] and transient isotachophoresis (tITP)[6,7] are often required prior to electrophoretic separation to improve limits of detection.[8,9] One significant challenge that hinders high sensitivity detection is the dispersion of sample zones (and accompanying reductions in signal strength) associated with transitioning from a preconcentration step to the CE step.[10,11]

An alternative to serial preconcentration-then-separation processes is employing electrophoretic focusing techniques which simultaneously preconcentrate and separate analytes, achieving a steady state signal with no further dispersion. Electrophoretic focusing techniques include temperature gradient focusing (TGF),[12,13] isoelectric focusing (IEF),[14] and electric field gradient focusing (EFGF).[15] These require fairly complex channel geometries and/or flow control methods and are not generally applicable to a wide range of analytes.

Isotachophoresis (ITP) is another preconcentration technique which leverages heterogeneous electrolytes (of varying electrophoretic mobility) to simultaneously preconcentrate and segregate analytes into non-dispersing zones.[16] In traditional analytical models, sample species segregate into distinct plateau-shaped (directly detectable) zones between trailing (TE) and leading electrolytes (LE).[16] These are detected directly with UV absorbance or conductivity detectors,[17,18] or can be detected indirectly with fluorescent mobility markers.[19] In contrast to plateau-mode ITP, sample species in very low initial concentrations result in so-called peak mode (or spike mode).[20] In typical peak mode, sample zones are not distinct and appear as peaks between the leading and trailing electrolyte zones.[20–22] The latter require an additional separation step to disrupt ITP and induce separation. The traditional methods accomplish this by replacement of the discontinuous LE-TE electrolyte system with a uniform electrolyte either by transient ITP (tITP) or column coupling.[23–26] In both approaches, the replacement of electrolytes results in electromigration dispersion (in addition to diffusion and advective dispersion) which partially offsets the signal improvement from ITP preconcentration itself.[27,28] A few ITP studies have addressed the problem of detecting peak-mode analytes by introducing non-detectable spacer ions (with mobilities intermediate to that of directly-detectable sample species of interest) to improve resolution.[29–31] The latter technique has been used exclusively for UV-absorbent/detectable analytes with non-UV absorbent/undetectable spacers and requires careful selection of spacer ions.

In this paper, we present a new separation method which achieves simultaneous preconcentration and separation in ITP with a simple, single-step sample injection. We propose and experimentally demonstrate that carbonate ions (and carbamate ions) resulting from dissolved atmospheric carbon dioxide (and its reaction with buffer species containing primary or secondary amines) weakly disrupt the ITP mode and induce separation of the analyte species. We show that this assay results in finite spacing of peak-mode analyte zones, despite the fact that there is no spacer of intermediate mobility introduced. Separation

Department of Mechanical Engineering, Stanford University, 440 Escondido Mall Bldg 530, room 225, Stanford, CA, 94305, USA. E-mail: juan.santiago@stanford.edu

† Electronic supplementary information (ESI) available: Detection of ITP zones with fluorescent counterion. See DOI: 10.1039/b815460k

This journal is © The Royal Society of Chemistry 2009

analogous to zone electrophoresis occurs simultaneously with ITP-type focusing of analyte species. We first present an experimental study on the influence of carbonate ions on the TE-LE interface shapes, and show results from various controlled experiments that verify the proposed separation mechanism. We then demonstrate example applications of this ITP technique to the separation of the DNA ladder and to the fractionation of DNA and proteins from a mixture.

Theory

Mechanism for simultaneous focusing and separation

In peak mode ITP, analytes accumulate at the interface between the LE and TE (order 10 μm wide) and appear as a single analyte peak to the (*e.g.*, fluorescence, conductivity, or absorbance) detector. Fig. 1a shows a typical example of two concentrated analyte zones, initially present in trace concentration, and merged within the TE-LE interface. However, when the ITP buffer system (*i.e.* the LE and TE) is "contaminated" with atmospheric carbon dioxide, we here show that the analyte zones

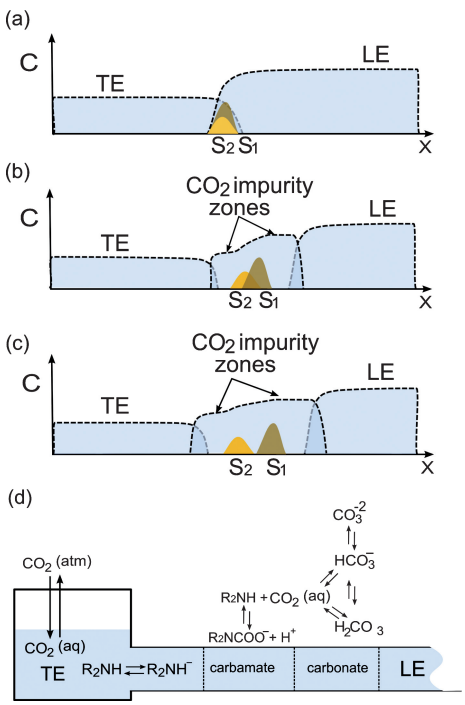

Fig. 1 Schematic of preconcentration and separation of analytes at the TE-LE interface *via* peak mode ITP. (a) Depicts a situation where the LE and TE buffers do not focus ions resulting from CO_2 or (an idealized situation) where the LE and TE do not contain dissolved carbon dioxide. Here, analytes (S_1 and S_2) with mobilities intermediate to LE and TE accumulate at the interface and do not separate. (b) The LE and TE buffers are "contaminated" with dissolved atmospheric CO_2 and carbonate (and/or carbamate) zones focus at the interface. An electric field gradient is generated. The analytes focus at locations corresponding to their local mobility. (c) Here, CO_2 impurity zones have grown wider with time and the electric field gradient region is wider. The spacing between analyte peaks also increases. (d) Schematic of various ITP zones resulting from reactions of CO_2 to form bicarbonate, carbonate and carbamate species.

gradually separate and yet remain focused. This is shown schematically in Fig. 1b and 1c. In case of non-finite analyte zone injection (*i.e.*, analytes added to the TE or LE), both accumulated moles[22] and the peak resolution increases with time. Hence, we achieve simultaneous preconcentration and separation of analyte zones without spacers or additional separation steps. We hypothesize that the separation occurs due to the interference of dissolved atmospheric carbon dioxide with the ITP preconcentration.

The current assay has characteristics consistent with a traditional ITP process including analyte zones which focus within a region of electric field gradient imposed by fast leading ions and slow trailing ions. Also, analyte peaks achieve a nearly steady state maximum concentration for a finite sample injection. However, the introduction of carbonate disturbances imparts slight velocity differences between peaks leading to separation. Unlike traditional ITP, the electric field gradient across the leading-trailing zone in the current assay is fairly wide spread (*e.g.*, has the width of 10 or more sample peak widths) and this assists in separation of analyte peaks which are simultaneously focused in this gradient region.

Most aqueous buffer solutions used in anionic ITP contain dissolved carbon dioxide due to its high solubility in aqueous solutions (*e.g.*, CO_2 is almost 50 times more soluble than nitrogen in water). Upon hydration, dissolved CO_2 forms carbonic acid which dissociates to form bicarbonate and carbonate ions depending on the pH of the system. The reaction scheme for hydration and dissociation reactions can be expressed as

$$CO_{2(aq)} + H_2O \underset{k_{21}}{\overset{k_{12}}{\rightleftharpoons}} H_2CO_3$$

$$H_2CO_3 \underset{k_{32}}{\overset{k_{23}}{\rightleftharpoons}} HCO_3^- + H^+$$

$$CO_{2(aq)} + OH^- \underset{k_{31}}{\overset{k_{13}}{\rightleftharpoons}} HCO_3^-$$

$$HCO_3^- \underset{k_{43}}{\overset{k_{34}}{\rightleftharpoons}} CO_3^{2-} + H^+$$

The thermodynamics and kinetics of these reactions have been extensively studied and details can be found in review articles by Kern[32] and Edsall.[33] The hydration of carbon dioxide occurs slowly (time scale $\tau \sim 10$ s) compared to the acid dissociation reaction ($\tau \sim 1$ μs). The carbonate (and bicarbonate) ions from dissociation of carbonic acid are well known to interfere with ITP zones in anionic ITP analysis.[34,35] In particular, for plateau mode ITP, the carbonate ions originating from the TE overspeed the analyte zones and result in diluted, and therefore wider analyte zones. The carbonate-ion-induced dilution and elongation of ITP zones has been experimentally studied by Hirokawa *et al.*[36]

Dissolved carbon dioxide also reacts with uncharged primary and secondary amine groups (*e.g.*, in various amines and amino acids) resulting in formation of carbamate ions. This reaction is also relevant to ITP systems since many anionic ITP analyses use an amino acid (such as glycine or ε-aminocaproic acid) as the trailing ion due to their high pK_a and associated low effective mobility. Commonly used buffering counterions in these systems

This journal is © The Royal Society of Chemistry 2009

also contain amine groups; including tris, bis-tris propane, alanine, benzylamine, and others. The reaction of amines with carbon dioxide was recognized and studied by Siegfried and Newmann[37] and Faurholt.[38]

$$RNH_2 + CO_{2(aq)} \underset{k_{51}}{\overset{k_{15}}{\rightleftharpoons}} RNHCOO^- + H^+$$

The equilibrium constants and kinetic rates for these carbamate formation reactions have been experimentally obtained for various amino acids and peptides.[39–43] The characteristic time scale for the forward reaction is ~0.1 s[42] and the typical value of equilibrium constant for amino acids is $\sim 1 \times 10^{-5}$.[44] Although the mechanism of carbamate ion formation is well known, the occurrence (and interference) of carbamate zones in ITP analyses has not, to our knowledge, been reported. We suspect that unknown species zones observed in many published ITP studies[45–48] employing amine containing buffers are in fact carbamate ion zones.

We hypothesize that the slow reaction kinetics of hydration of carbon dioxide and carbamation of primary and secondary amines result in electric field gradients at the interface of carbonate and carbamate zones. Fig. 1d shows a schematic of carbonate and carbamate zones formed between the LE and TE interface along with the various equilibrium reactions that occur in these zones. The interface gradients and associated separation phenomenon cannot be captured by any of the ITP simulation tools available today (*e.g.*, SIMUL[49]). The current models assume instantaneous equilibrium reactions and fail to capture finite reaction rate kinetics and its coupling with ITP. Indeed, there is a dearth of ITP studies on the effect of reaction kinetics on ITP dynamics; one notable exception is the work of Gebauer and Bocek *et al.*[50] who presented a theoretical treatment of slow reaction kinetics between cations and complexing counterions in cationic ITP and the resulting electrodiffusion at ITP boundaries. We hypothesize that analogous electrodiffusion phenomena due to slow reaction kinetics occur with carbamate and carbonate zones and result in formation of electric field gradients across the interface. The analyte zones (in peak mode ITP) experience this electric field gradient (*c.f.*, Fig. 1b and 1c) and therefore, focus at various locations in the gradient region as dictated by their effective electrophoretic mobility. We present experimental evidence in later sections to corroborate our hypothesis.

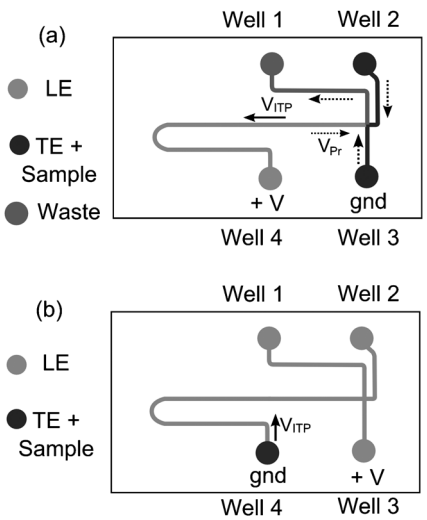

Fig. 2 Schematic of the injection protocol for establishing a single ITP interface on a microfluidic chip. (a) The TE-LE interface is set up at the channel intersection by applying vacuum on well 1 after loading wells 2, 3 with TE and well 4 with LE. The pressure-driven-flow velocity is indicated by a dotted arrow and electromigration velocities V_{ITP} are shown with solid arrow. (b) A TE-LE interface can alternately be established at the entrance to well 4 and high voltage is applied across wells 3 and 4 to initiate ITP.

Experimental

We performed single interface ITP experiments to study the development of the TE-LE interface and the preconcentration and separation of the analytes. All experiments were performed in a Caliper NS-95A chip with channel dimensions 34 μm wide by

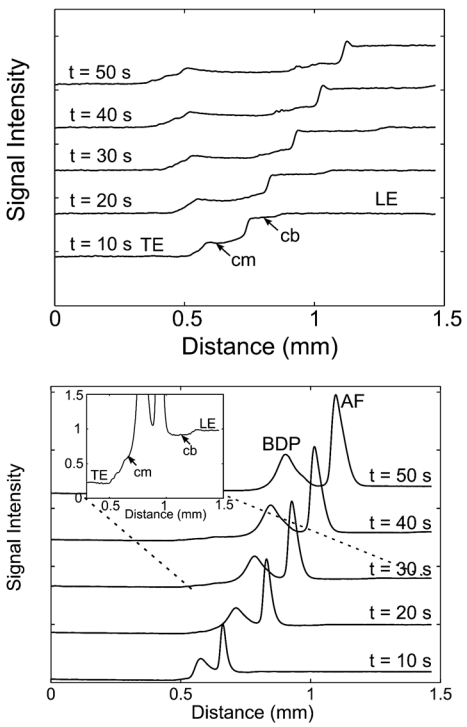

Fig. 3 (a) Fluorescence intensity (width averaged intensity from image data) within the separation microchannel at five instances 10 s apart, for a single interface ITP experiment with 200 mM BisTris HCl (pH = 6.4) as the leading electrolyte and 100 mM glycine titrated with 20mM NaOH (pH = 9.1) as the trailing electrolyte. 10 μM Rhodamine 6G was added to the LE to serve as a tracer to visualize the electric field throughout all zones (high signal indicates low electric field). The interface between the TE-LE contains two plateau zones, carbonate (cb) and carbamate (cm) with a gradient region between them. The carbonate, carbamate (and gradient) regions grow wider with time due to their continuous influx from the TE zone. (b) Fluorescence intensity within the microchannel at five different times in another experiment with identical experiment conditions, but with the addition of two anionic fluorescent analytes BODIPY and Alexa Fluor 488. Analytes were added to the TE and focus at the interface region between LE and TE. The analytes gradually separate as the carbamate and carbonate interface regions grow wider.

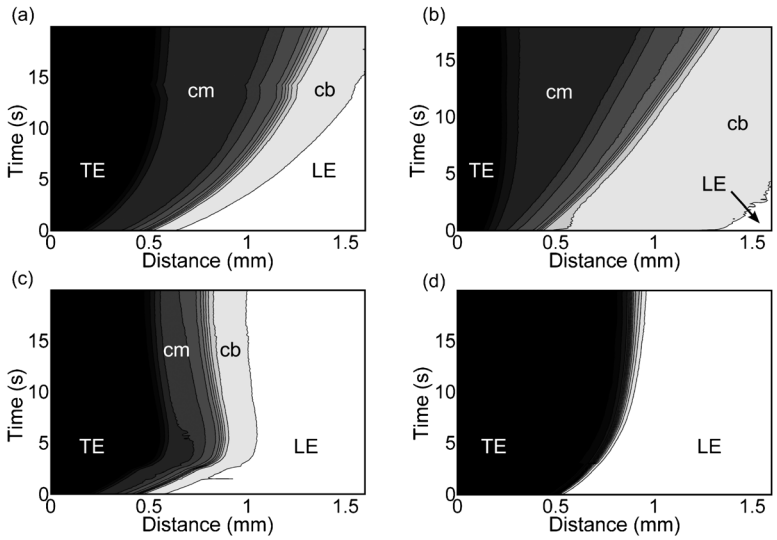

Fig. 4 Spatiotemporal plots of the TE-LE interface in single interface ITP experiments visualized with a fluorescent counterion (Rhodamine 6G). The four plots correspond to four experiments with different TE buffer compositions. The LE consisted of 200 mM BisTris HCl and the TE contained 250 mM bis-tris glycine in all four cases. Case (a) shows the development of carbamate (cm) and carbonate (cb) zones for the given TE-LE (a control case). In (b), 2 mM sodium bicarbonate was added to the TE and we observed wider carbamate and carbonate zones. In (c) 5 mM barium hydroxide was added to the TE well ~15 s after the start of the experiment (at $t = 5$ s in the plot). Upon application of barium hydroxide, the interface quickly establishes a constant width. In case (d), barium hydroxide was added to the TE before starting the experiment and the carbonate and carbamate zones do not appear.

12 μm deep (in the separation channel). A schematic of the chip is shown in Fig. 2a. Briefly, we load well 4 with the LE and wells 2 and 3 with the TE (with or without the sample). We then apply vacuum at well 1 to fill the separation channel with LE; and the TE-LE interface is established at the intersection of the chip as shown. To initiate ITP stacking, high voltage (600 V) is applied across wells 3 and 4 and the interface migrates towards well 4. We then manually move a microscope optical stage to monitor the interface and acquire images at the various locations downstream of the simple cross-intersection. For the experiment requiring visualization of the TE-LE interface over long times (~100 s, *c.f.* Fig. 3, 4 and 5), we use pressure-driven counterflow to keep the interface approximately stationary by applying a vacuum to well 1.

Fig. 2b shows an alternate injection protocol (used here in the experiments of Fig. 7 and 8) which achieves one step preconcentration and separation in a single channel (or capillary). The channels are filled with LE and the initial TE-LE interface is established at the inlet of well 4. The analyte species are added to the TE in well 4 and high voltage is applied across wells 3 and 4 to initiate simultaneous ITP preconcentration and separation.

We prepared 1M stock solutions of various LE (tris, bis-tris) and TE (glycine, HEPES, TES, taurine) species and diluted them to the desirable concentrations specified in the respective sections. The LE and TE also contained 2% polyvinyl pyrrolidone (PVP) to suppress electroosmotic flow. In a few control experiments described later, we also added $Ba(OH)_2$ (100 mM stock solution) to precipitate dissolved carbon dioxide. The LE and TE reagents were obtained from Sigma-Aldrich (St. Louis, MO). The fluorescent analytes Alexa Fluor 488, fluorescein, and BODIPY were obtained from Invitrogen (Carlsbad, CA). We prepared 100 μM concentration stock solutions of these fluorescent analytes and diluted their final concentration to 100 nM

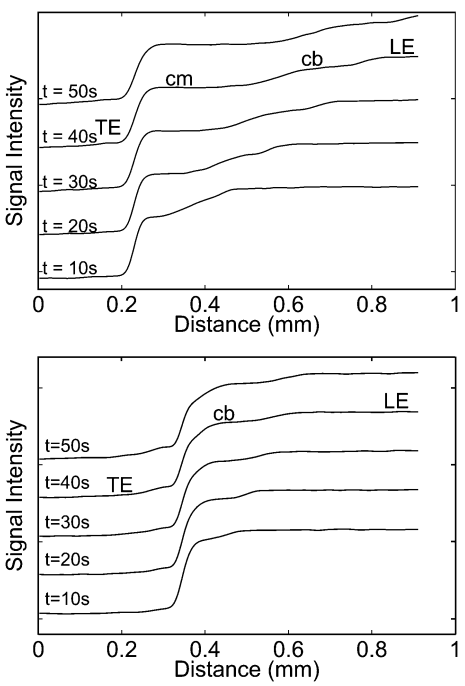

Fig. 5 Fluorescence intensity inside the microchannel at five time instants 10 s apart, for two single interface ITP experiments. High intensity indicates low local electric field. In case (a), the TE contained 100 mM TES (titrated with 40 mM NaOH to pH = 7.3) and the LE was 200 mM BisTris HCl. Here we observe carbonate (cb) and carbamate (cm) zones growing between the LE and TE zones. In case (b), the TE was changed to 50 mM HEPES (titrated with 20 mM NaOH to pH = 7.3) and only carbonate zone (cb) appears.

This journal is © The Royal Society of Chemistry 2009

in the TE. The 25 bp DNA ladder was obtained from Promega (Madison, WI), and fluorescent proteins green fluorescent protein (GFP), and allophycocyanin (ACN) were obtained from Invitrogen. We used 10X SYBR green, added to the LE, to visualize the DNA peaks with the epifluorescent detection setup. All solutions were prepared using ultra-filtered deionized water (DIUF) from Fischer Scientific (Fair Lawn, NJ).

For the experiments requiring visualization of the evolution of TE-LE interface, we added a fluorescent counterion (10 μM Rhodamine 6G) to the LE. The concentration (and therefore emitted intensity) of this fluorescent counterion adapts itself according to the local electric field in ITP zones (in accordance with mass conservation across interfaces as described in the ESI†). This indirect detection technique provides an indirect visualization of electric field distribution, and was first described by Chambers and Santiago.[51]

For imaging, we used an inverted epifluorescent microscope (IX70, Olympus, Hauppauge, NY) with a mercury lamp and a 10X (NA = 0.4) UPlanApo objective. We used a dual band filter cube (51006, Chroma) for imaging Rhodamine 6G and Alexa Fluor; or Fluorescein and Bodipy simultaneously. For other experiments (including DNA and protein separations), we used U-MWIBA filter-cube from Olympus (460–490/505/515 nm). Images were captured using a 12 bit, 1300 × 1030 pixel array CCD camera (Coolsnap, Roper Scientific, Trenton NJ) externally triggered using an Agilent function generator. We used a Labsmith high voltage supply (HVS 3000D) to initiate ITP stacking (0.5–2 kV).

Results and discussion

Separation by an electric field gradient within carbonate and carbamate zones

We first present experiments showing transient development of carbonate (and carbamate, when buffers contain primary or secondary amines) at TE-LE interfaces; and their effect on analyte peaks accumulated at the interface via peak mode ITP. To visualize the varying electric field profile through the TE-LE interface, we used the aforementioned indirect fluorescence detection technique. (We added Rhodamine 6G, a cationic dye with pK_a 7.5, to the LE at a trace concentration of 30 μM.)

In Fig. 3a, we show the fluorescence intensity of Rhodamine 6G across the LE and the TE zone obtained at various times for a single interface ITP experiment with 200 mM BisTris HCl (pH 6.4) as LE and 100 mM glycine (titrated with 20 mM NaOH to pH = 9.1) as TE. We applied 600 V across wells 3 and 4; and used counterflow by applying vacuum on well 1 to hold the ITP interface approximately stationary at x = 1.5 mm from the channel intersection. The data shows two "background" zones which increase in width with time, and the conductivity (or electric field) gradient through these zones grows shallower as these regions widen. As we shall see, these regions are (from TE to LE) the carbonate and carbamate zones.

Next, we added anionic fluorophores BODIPY and Alexa Fluor 488 (~100 nM concentration each) as sample fluorescent species to the TE and observed their focusing within the carbonate and carbamate field gradient region. In Fig. 3b, we show the typical resulting fluorescence intensity profiles. The background counterion tracer again shows the background zones, while the fluorescent peaks show the position and shape of the analyte zones. The analytes focus in the region within the carbonate and carbamate zones, as in Fig. 3b. As the carbonate and carbamate zones widen, the electric field gradient becomes less steep. The locations of analyte peak focii therefore move apart, resulting in effective separation between analyte peaks. Since the analytes are continuously being fed from the TE well (within the time scale of the experiment), their concentration also increases with time. We therefore observe simultaneous pre-concentration and separation in the assay.

Validation of presence of carbonate and carbamate: control experiments

Next, we present a series of experiments that validate our hypothesis that the carbonate ions (from dissolved atmospheric carbon dioxide) result in the formation of carbamate and carbonate zone and an electric field gradient at the TE-LE interface. In these experiments, we added 5 mM barium hydroxide ($Ba(OH)_2$) to the trailing electrolyte to precipitate the carbonate ions. Barium hydroxide is a strong base that precipitates carbonic acid out of the solution as barium carbonate due to its low solubility. Barium hydroxide is for this effect commonly added to TE.[52,53]

We present our control experiments, with and without barium hydroxide in the TE in the spatiotemporal plots in Fig. 4a–d. Here, the LE was 200 mM BisTris HCl and the TE contained 250 mM glycine (titrated with 250 mM BisTris) in all four cases shown. For visualization of the TE-LE interface, we added 10 μM Rhodamine 6G to the LE. No other focusing (fluorescent) analyte was present. We here also applied a counterflow to slow down the migration of the TE-LE interface. Fig. 4a shows the typical growth of the TE-LE interface as seen from the widening gray region between the LE zone (white region) and TE zone (black). Again, we observe two distinct intermediate zones (carbonate and carbamate) between the leading and trailing zones. In Fig. 4b, we added 2 mM $NaHCO_3$ to the TE to visualize the effect of additional carbonate ions in the TE. Here, as expected with addition of a source of carbonate ions, the (carbonate and carbamate) interface regions between the TE and LE grow significantly more rapidly. For example, compare the increase with that of the carbonate zone at 5 s, and the increased width of the carbamate zone at 15 s.

For the experiment shown in Fig. 4c, we added barium hydroxide to the TE zone after the interface has arrived at the detector location (at ~t = 5 s in the plot). We see the pressure disturbance caused by the (real-time) dispensing of barium hydroxide into the TE well, appearing as a momentarily wavy trace in the plot. As expected in the addition to this strong carbonate scavenger, the interface width is "frozen" thereafter. (The carbamate and carbonate zones remained the width even after 60 s). Finally, Fig. 4d shows the spatiotemporal plot for the case when barium hydroxide was added to the TE before the experiment was started. Barium hydroxide effectively removes dissolved CO_2 and carbonate ions from the TE, and so we do not observe intermediate carbamate and carbonate zones. As expected, and again consistent with our hypothesis, the TE-LE interface remains very sharp and does not grow with time.

These experiments validate our hypothesis that the carbonate ions from the TE well interfere with ITP dynamics and cause the TE–LE interface to increase in width. We also observe the effect of these "impurity" species on the conductivity field (and therefore, electric field) within the carbonate and carbamate zones. We confirmed our hypothesis with a series of other experiments not described here. For example, in experiments with one or more fluorescent analytes, addition of barium hydroxide to the TE at the start of the experiment consistently and uniformly resulted in no separation of analytes (as in Fig. 1a).

Carbamate zone formation

Carbarmate ions result from the reaction of primary or secondary amine groups with carbon dioxide.[54] Even though the reaction mechanism and kinetics of carbamate formation is well studied, the occurrence of carbamate zones in ITP has to our knowledge never been reported. We verified the presence of carbamate zones by performing series of experiments comparing TE chemistries. We here summarize one such typical study comparing HEPES and TES as trailing ions. The pK_a and fully-ionized mobilities of these two species are nearly identical and hence their electromigration behavior is expected to be very similar. However, TES contains a secondary amine group and we expect it to form carbamate species, whereas HEPES possesses only a tertiary amine group and hence does not form carbamate.

Fig. 5 shows the TE-LE interface profile approximated from the fluorescence intensity of Rhodamine 6G for these two experiments. The LE in Fig. 5a–b consisted of 200 mM BisTris HCl. In Fig. 5a–c, the TE was 100 mM TES titrated with 40 mM NaOH. Here, we observe two intermediate zones between the LE and TE zones: carbonate and carbamate. These zones, and the dispersed interface they form, grow wider with time as seen from the fluorescence intensity profiles at various time instants. Fig. 5b is a negative control experiment for the presence of the carbamate zone. In the latter experiment, the TE consisted of 50 mM HEPES titrated with 20 mM NaOH. Here, only the carbonate zone is formed between the LE and TE as HEPES does not form carbamate with CO_2.

The simultaneous focusing and separation of the analytes is analogous to other electric field gradient focusing techniques.[15,55] However, in the current ITP assay, the electric field gradient is autogenously generated at the interface due to the combined effects of ITP and finite-rate reaction kinetics. In order to validate that electric field gradient plays a pivotal role in the both focusing and resolving/separating analytes in our assay, we varied the applied voltage in the experiment and observed the change in shape of the analyte peaks. We present a result from one such validation experiment in Fig. 6. Here, we show the spatio-temporal plot of focusing and separation of three analytes: Alexa Fluor 488, Fluorescein and BODIPY focused between the LE (tris HCl at 150 mM, pH = 8.1) and the TE (tris taurine at 100 mM initial concentration, pH = 8.6). Initially, 200 V is applied at the LE well and the TE well is grounded. The analyte zones are wider and poorly resolved under these conditions and the zones migrate slowly as seen from the slope of the trace of analyte zones in first 5 s of the spatio-temporal plot. At a later instant (t = 5 s), the LE well voltage is rapidly raised to 800 V and the analyte zones become narrower and are thereafter well

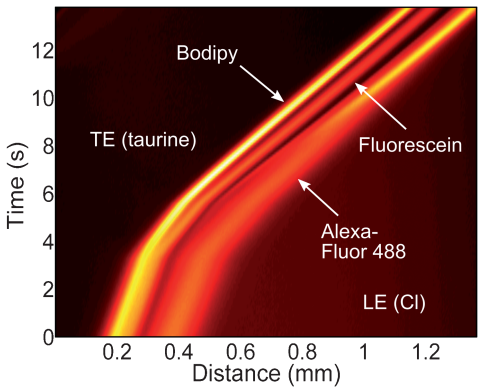

Fig. 6 Spatio-temporal plot showing the dynamics of the focused analyte zones in response to the sudden increase in the electric field in a single interface ITP experiment. Here, the LE was 150 mM tris HCl (pH = 8.1) and TE was 100 mM tris taurine (pH = 8.6). The applied voltage is changed rapidly from 200 to 800 V at t = 5 s. In response, the analyte bands focus into narrower peaks and migrate at higher velocity (indicated by the decreased slope of the traces).

resolved. Analyte zones now migrate at higher (but still identical) velocity as indicated by the equal slope of their three respective fluorescent traces. This simple experiment highlights the importance of the interplay between focusing rate (determined by electric field strength and gradient) and dispersion forces (here dominated by molecular diffusion). Analyte peak width and resolution are determined by a balance between electromigration and diffusion, and under low electric field conditions diffusion flux dominates resulting in low concentrations and poor resolution.

Example applications of assay

While the presence of carbonate zones typically has undesirable effects on the focusing efficiency of ITP preconcentration assays[22] (due to widening the interface widths), they can be used to improve various other on-chip CE assays. One obvious advantage is that both preconcentration and separation of analytes are achieved simultaneously and there is no need for additional buffer exchange steps (*e.g.*, as in tITP). Also, what this assay achieves is easily implemented on standard capillary systems (without column coupling) and in single, straight microchannel architectures (*e.g.*, with no cross or double-T patterns) with a single loading step. We here demonstrate simultaneous preconcentration and separation of standard DNA and protein samples in such simple channels where we form the initial TE-to-LE interface at the entrance to the TE well.

We first present sample preconcentration and separation dynamics of a 25 bp DNA ladder consisting of 12 different DNA fragments. We used 50 mM Tris HCl as LE and 25 mM Tris glycine as TE. Under low ionic strength conditions (as chosen here), the DNA fragments are believed to experience reduced electrostatic shielding[56] and therefore exhibit greater differences in their electrophoretic mobilities in the presence of a sieving matrix. We used 1.5% Hydroxyethyl cellulose (added to the LE) as the sieving matrix and 1% PVP for EOF suppression. For visualization of the DNA bands, we added 10X SYBR Green to the LE. The DNA ladder was diluted 1000 fold in the TE to a final concentration of 0.36 ng μl^{-1}. In this experiment, we used

This journal is © The Royal Society of Chemistry 2009

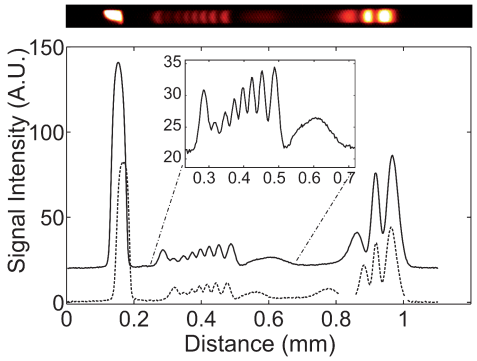

Fig. 7 The pseudo-colour image (top) and corresponding fluorescence intensity plots for the separation and preconcentration of 25 bp DNA ladder in single interface ITP experiment is shown. The LE and TE were 50 mM Tris HCl and 25 mM Tris glycine, respectively. The solid and dotted curves show the fluorescence intensity after the peaks have migrated 15 mm and 25 mm, respectively, from the initial TE-LE interface location. The fluorescence intensity increases due to preconcentration *via* ITP and the resolution also increases with the distance travelled by the interface.

a single channel injection protocol as described in Fig. 2b. Fig. 7 shows the pseudo-color image of the separated DNA peaks and the corresponding (simple width-averaged axial) fluorescence intensity plots obtained 15 mm and 25 mm downstream of the initial TE-LE interface location. The DNA bands simultaneously separate and preconcentrate (see width-average intensity plots). The fluorescence intensity of the DNA bands increases as it migrates downstream due to the accumulation of the DNA sample. The resolution of the DNA bands also increases with time. The relative spacing between the DNA peaks changes (*e.g.* peak 4 and peak 5 from right are shifted in Fig. 7) since the electric field gradient between LE and TE zones becomes shallower with time and the focus point for the analyte peak therefore changes.

From the spatiotemporal plot of the migration of DNA bands shown in Fig. 8, we observe that the DNA bands migrate at

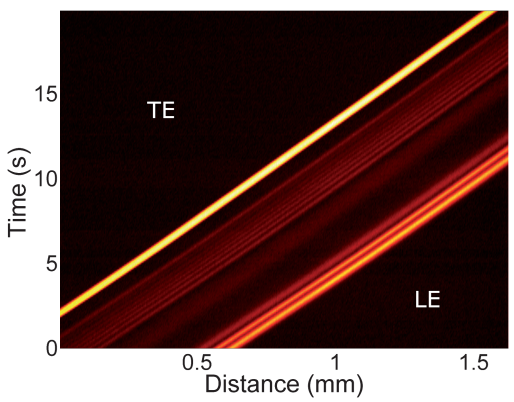

Fig. 8 Spatio-temporal plot of migration of DNA bands in a 25 bp DNA ladder separated and preconcentrated *via* single interface ITP (same conditions as in caption of Fig. 7). The parallel traces of DNA bands indicate that the bands migrate at nearly constant speed as per the ITP condition. The bands slowly separate over longer (~1 cm) distances as the interface regions between TE-LE grow wider from the effect of slow reaction rates of carbamate and carbonate ions.

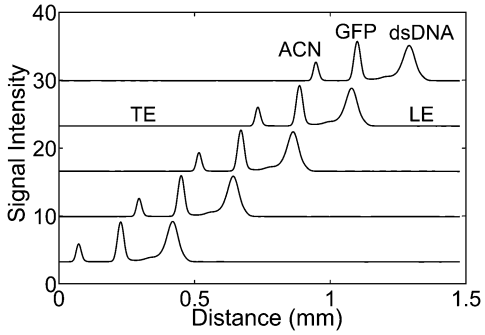

Fig. 9 Electropherograms for simultaneous preconcentration and separation of 25 bp DNA ladder from green fluorescent protein (GFP) and allophycocyanin (ACN) in a single interface ITP experiment with 50 mM Tris HCl as the LE and 100 mM Tris glycine as the TE. The electropherograms are obtained at various time instants (each 4 s apart) and the separated analyte peaks remain focused and dispersion-free as they migrate downstream.

nearly the same velocity and that the ITP mode persists (*i.e.*, the bands are not dispersing). This is strong evidence that the ITP condition is only weakly violated by the overspeeding and transient accumulation of carbonate species here. The resolution and optimization of such DNA assays is ongoing work which we will present in future work.

The current focusing and separation technique can also be used in fractionation assays to extract an analyte from a mixture. Fig. 9 shows preconcentration and separation of 25 bp DNA ladder and two proteins GFP (green fluorescent protein) and allophycocyanin (ACN) from their mixture *via* one step ITP separation. Here, the LE was 50 mM Tris HCl (pH 8.1) and TE was 100 mM Tris glycine. We here injected a 4 mm long injection zone which included the DNA ladder, GFP, and ACN diluted in the TE. The LE contained 1% PVP for EOF suppression and did not contain a sieving matrix (*e.g.* HEC), so DNA peaks did not separate and migrated as a single peak. Fig. 9 shows typical resulting electropherograms from the separation at times 4 s apart. The separated peaks remain focused and free of dispersion. Such experiments demonstrate the possibility of using single interface ITP in simple, straight channels for fractionation assays.

Conclusion

We have demonstrated a separation method which achieves simultaneous preconcentration and separation in single interface ITP. Unlike previous ITP studies that require electrophoretic spacers or ampholytes, we leveraged ions resulting from dissolved atmospheric carbon dioxide to achieve simultaneous focusing and separation. We proposed a mechanism for the separation of analytes due to the migration and accumulation of carbonate and carbamate ions; and presented various control experiments for validation. Carbon dioxide hydration has slow reaction kinetics and subsequent carbonate ions have high electrophoretic mobility; and so carbonate zone appears behind LE ions. The dissolved carbon dioxide also reacts with ITP buffers containing primary or secondary amines to form carbamate ions that overspeed and accumulate just ahead of the TE. The slow reaction kinetics and carbonate overspeeding effects result in the

formation of an electric field gradient in the region between the LE and TE zone. The width of this gradient region increases over time, and analytes focus within it at locations determined by their electrophoretic mobility.

We have used this separation mechanism to simultaneously preconcentrate and separate analytes *via* single interface isotachophoresis. We demonstrated separation of a standard 25 bp DNA ladder with this assay and obtained well resolved, dispersion-free DNA peaks. As a demonstration of the fractionation capabilities of the assay, we have also shown extraction of a DNA ladder and two proteins, GFP and allophycocyanin from initial mixture. In all cases, separated peaks remain focused for a long duration (and separation distance), so they can be recovered downstream of the channel for further analysis.

Acknowledgements

We gratefully acknowledge support from the Micro/Nano Fluidics Fundamentals Focus (MF3) Center funded by Defense Advanced Research Projects Agency (DARPA) MTO Grant No. HR0011-06-1-0050 and contributions from MF3 corporate members. We also gratefully acknowledge the support of the DARPA MTO sponsored SPAWAR Grant N66001-09-1-2007.

References

1 K. D. Altria, *J. Chromatogr., A*, 1999, **856**, 443–463.
2 V. Dolník, S. Liu and S. Jovanovich, *Electrophoresis*, 2000, **21**, 41–54.
3 D. S. Burgi and R. L. Chien, *Anal. Chem.*, 1991, **63**, 2042–2047.
4 B. Jung, R. Bharadwaj and J. G. Santiago, *Electrophoresis*, 2003, **24**, 3476–3483.
5 P. E. Jackson and P. R. Haddad, *Trends Anal. Chem.*, 1993, **12**, 231–238.
6 P. Gebauer, Z. Mala and P. Bocek, *Electrophoresis*, 2007, **28**, 26–32.
7 M. Urbanek, L. Krivankova and P. Bocek, *Electrophoresis*, 2003, **24**, 466–485.
8 R. Chien, *Electrophoresis*, 2003, **24**, 486–497.
9 S. C. Jacobson and J. M. Ramsey, *Electrophoresis*, 1995, **16**, 481–486.
10 L. Krivánková, P. Gebauer, W. Thormann, R. A. Mosher and P. Bocek, *J. Chromatogr., A*, 1993, **638**, 119–135.
11 G. O. Roberts, P. H. Rhodes and R. S. Snyder, *J. Chromatogr., A*, 1989, **480**, 35–67.
12 D. Ross and L. E. Locascio, *Anal. Chem.*, 2002, **74**, 2556–2564.
13 D. E. Huber and J. G. Santiago, *Electrophoresis*, 2007, **28**, 2333–2344.
14 A. E. Herr, J. I. Molho, K. A. Drouvalakis, J. C. Mikkelsen, P. J. Utz, J. G. Santiago and T. W. Kenny, *Anal. Chem.*, 2003, **75**.
15 W. S. Koegler and C. F. Ivory, *J. Chromatogr., A*, 1996, **726**, 229–236.
16 A. J. P. Martin and F. M. Everaerts, *Anal. Chim. Acta*, 1967, **38**, 233–237.
17 P. Bocek, M. Deml, P. Gebauer and V. Dolnik, *Analytical Isotachophoresis*, VCH, New York, 1988.
18 F. M. Everaerts, J. L. Beckers and T. P. E. M. Verheggen, *Isotachophoresis: Theory, Instrumentation, and Applications*, New York, Amsterdam, 1976.
19 T. K. Khurana and J. G. Santiago, *Anal. Chem.*, 2008, **80**, 279–286.
20 M. Svoboda and J. Vacik, *J. Chromatogr., A*, 1976, **119**, 539–547.
21 P. Gebauer and P. Bocek, *Electrophoresis*, 1995, **16**, 1999–2007.
22 T. K. Khurana and J. G. Santiago, *Anal. Chem.*, 2008, **80**, 6300–6307.
23 F. Foret, V. Sustacek and P. Bocek, *J. Microcolumn Sep.*, 1990, **2**, 229–233.
24 F. Foret, E. Szoko and B. L. Karger, *Electrophoresis*, 1993, **14**, 417–428.
25 L. Krivankova, P. Gebauer and P. Bocek, *J. Chromatogr., A*, 1995, **716**, 35–48.
26 C. Schwer, B. Gas, F. Lottspeich and E. Kenndler, *Anal. Chem.*, 1993, **65**, 2108–2115.
27 V. Sustácek, F. Foret and P. Bocek, *J. Chromatogr., A*, 1991, **545**, 239–248.
28 M. Urbánek, M. Pospísilová and M. Poláscaronek, *Electrophoresis*, 2002, **23**, 1045–1052.
29 F. Oerlemans, C. Debruyn, F. Mikkers, T. Verheggen and F. M. Everaerts, *J. Chromatogr., B*, 1981, **225**, 369–379.
30 I. Nagyova and D. Kaniansky, *J. Chromatogr., A*, 2001, **916**, 191–200.
31 S. Husmann-Holloway and E. Borriss, *Fresenius' J. Anal. Chem.*, 1982, **311**, 465–466.
32 D. M. Kern, *J. Chem. Educ.*, 1960, **37**, 14–23.
33 J. T. Edsall, *CO2: Chemical, Biochemical, and Physiological Aspects*, NASA SP-188, ed. Robert E. Forster, John T. Edsall, Arthur B. Otis and F. J. W. Roughton, 291, 1969.
34 T. P. E. M. Verheggen, J. C. Reijenga and F. M. Everaerts, *J. Chromatogr., A*, 1983, **260**, 471–477.
35 P. Bocek and P. Gebauer, *Electrophoresis*, 1984, **5**, 338–342.
36 T. Hirokawa, T. Taka, Y. Yokota and Y. Kiso, *Journal of Chromatography*, 1991, **555**, 247–253.
37 M. Siegfried and C. Neumann, *Hoppe-Seylers Zeitschrift Fur Physiologische Chemie*, 1908, **54**, 423–436.
38 C. Faurholt, *J. Chim. Physique*, 1925, **22**, 1–44.
39 D. E. Penny and T. J. Ritter, *J. Chem. Soc., Faraday Trans. I*, 1983, **79**, 2103–2109.
40 W. C. Stadie and H. O'Brien, *J. Biol. Chem.*, 1936, **112**, 723–758.
41 F. J. Roughton and L. Rossiber, *Proc. R. Soc. London, B*, 1966, **164**, 381, –&.
42 J. R. Chipperfield, *Proc. R. Soc. London, B*, 1966, **164**, 401–410.
43 M. Caplow, *J. Am. Chem. Soc.*, 1968, **90**, 6795, –&.
44 J. G. Chen, M. Sandberg and S. G. Weber, *J. Am. Chem. Soc.*, 1993, **115**, 7343–7350.
45 D. Kaniansky, E. Simunicova, E. Ölvecká and A. Ferancová, *Electrophoresis*, 1999, **20**, 2786–2793.
46 J. E. Prest, S. J. Baldock, P. R. Fielden, N. J. Goddard, S. Mohr and B. J. Treves Brown, *J. Chromatogr., A*, 2006, **1119**, 183–187.
47 J. E. Prest, S. J. Baldock, P. R. Fielden, N. J. Goddard and B. J. Treves Brown, *J. Chromatogr., A*, 2003, **990**, 325–334.
48 J. E. Prest, S. J. Baldock, P. R. Fielden, N. J. Goddard and B. J. Treves Brown, *J. Chromatogr., A*, 2004, **1051**, 221–226.
49 V. Hruska, M. Jaros and B. Gas, *Electrophoresis*, 2006, **27**, 984–991.
50 P. Gebauer and P. Bocek, *J. Chromatogr.*, 1984, **299**, 321–330.
51 R. Chambers and J. G. Santiago, *Anal. Chem.*, DOI: 10.1021/ac60147a030/.
52 The LE well also contains carbonate ions, but we add no barium hydroxide there as carbonate ions electromigrate toward the cathode; and barium ions would enter all ITP zones, changing ITP dynamics by inducing greater dissociation of analytes, influencing migration order, etc. Also, we wish to avoid entrainment of barium carbonate precipitant particles into the channel entrance *via* electroosmosis, which may cause undesirable effects such as clogging.
53 C. J. Holloway and V. Pingoud, *Electrophoresis*, 1981, **2**, 127–134.
54 M. M. Sharma, *Trans. Faraday Soc.*, 1965, **61**, 681–688.
55 C. F. Ivory, *Sep. Sci. Technol.*, 2000, **35**, 1777–1793.
56 E. Stellwagen and N. C. Stellwagen, *Biophys. J.*, 2003, **84**, 1855–1866.

 This journal is © The Royal Society of Chemistry 2009